THE ASTROPHYSICAL JOURNAL, 391:443–452, 1992 June 1

TRACING LARGE-SCALE FLUCTUATIONS BACK IN TIME

ADI NUSSER AND AVISHAI DEKEL
Racah Institute of Physics, The Hebrew University of Jerusalem, Jerusalem 91904, Israel; and
D.A.E.C., Observatoire de Paris-Meudon, 92195 Meudon Cedex, France
Received 1991 August 9; accepted 1991 November 20

ABSTRACT

We present and test a quasi-linear method for recovering the growing mode of the initial fluctuations of a cosmological gravitating system from the present large-scale peculiar velocity or density field. First, a velocity-potential field is extracted from the observed velocities as in the POTENT procedure, or from the density as in the analysis of *IRAS* redshift surveys, assuming that the velocity field, smoothed on a scale of a few megaparsecs, is irrotational. Then, assuming the Zel'dovich approximation with no orbit crossing, the potential is traced back in time by integrating a simple differential equation in Eulerian space—the *Zel'dovich-Bernoulli* equation. Finally, the linear velocity and density fields are computed from the linear potential by differentiation. A correction factor for the effect of smoothing velocities over many streams is derived empirically from simulations.

The method is demonstrated to reconstruct the initial conditions of an N-body simulation, recovering in particular the initial Gaussian distribution of densities; the initial hills are lower and the valleys are deeper than predicted by linear theory. As an illustration of a possible application we present maps of the initial density field in our local cosmological neighborhood based on the POTENT and *IRAS* analysis.

Subject headings: cosmology: theory — dark matter — galaxies: clustering — gravitation — large-scale structure of universe — methods: numerical

1. INTRODUCTION

Given the nonlinear large-scale structure observed today, it could be very rewarding if one could trace it back in time through the gravity era to recover the linear fluctuation fields of density, velocity, and gravitational potential at $z \sim 10^3$. These linear fields would allow a more direct comparison with theory, which involves the origin of the fluctuations and the nature of the dark matter, and they are directly related to the fluctuations in the microwave background (e.g., Bertschinger, Gorski, & Dekel 1990).

In the standard framework for the formation of large-scale structure, the present structure, smoothed on large enough scales, is assumed to have grown via gravitational instability from small energy-density fluctuations that originated in the early universe. In linear theory, assuming dust, the power spectrum of the fluctuations evolves at a universal rate on all scales (e.g., Peebles 1980), but the dominance of radiation until $z \sim 10^4$ and the coupling of matter and radiation until $z \sim 10^3$ introduce nontrivial filtering which depends on the nature of the (dark) matter (e.g., being baryonic, "cold" or "hot"). So the linear spectrum at $z \sim 10^3$ contains important theoretical information.

However, the nonlinear gravitational evolution at recent epochs ($0 < z < 10$, say) "contaminates" the linear fluctuations of interest, even on scales of order $10h^{-1}$ Mpc and more, in a way that could not in general be reproduced by simple analytical means. The standard way of solving the nonlinear differential equations governing the evolution of fluctuations (the continuity, Euler, and Poisson equations) is by performing numerical simulations.

Why can't we integrate these equations back in time? Why can't we simply reverse the time in our N-body codes and run them backwards? After all, gravity is time-reversal invariant, and there is nothing in the equations that distinguishes t from $-t$ (the time symmetry is broken only by the fact that the universe appears to be presently expanding).

The situation is really hopeless for collapsed, virialized systems, where most memory has practically been erased. For example, when a particle is orbiting a galaxy or a cluster, there is no way to tell how times it has been around its orbit since its first infall and capture. There are many different initial conditions that can result in an almost identical final system.

But the situation is problematic even for linear systems. Recall that the linear solution for the density fluctuations has a growing mode [$D_1(t) \propto t^{2/3}$] and a decaying mode [$D_2(t) \propto t^{-1}$] (Peebles 1980, eq. [11.7], assuming matter-dominance, $p = \Lambda = 0$ and $\Omega = 1$). The decaying mode is likely to have left no detectable trace in the present universe. But when one attempts to integrate the equations backward in time, the D_2 mode picks up noise in the present fields, or numerical errors, and it amplifies them into artificial fluctuations of high amplitude which eventually dominate the density and velocity fluctuations at early times. This procedure has a negligible probability of recovering the very special state, of almost uniform density and tiny velocities, which we assume for the real universe at early times—there is much more phase space in clumpy, hot states. Thus, thermodynamics is responsible for breaking the time reversability of the problem; it prevents us from simply integrating the equations back in time.

In order to operate a gravitational time machine one must therefore control the decaying modes or eliminate them altogether. One way to do this is by using the Zel'dovich approximation (Zel'dovich 1970) which is naturally restricted to the evolution of the growing mode.

The Zel'dovich model provides a simple and successful quasi-linear scheme for following the motion of mass particles in an expanding universe. It is usually formulated in terms of the Lagrangian coordinates attached to particles, whose pecu-

liar velocities are assumed to evolve according to a universal function of time. Given the present positions and velocities of a set of test particles one could use the Lagrangian Zel'dovich formalism to obtain the initial positions and velocities of these particles. The initial velocities could then be interpolated into a grid to give the desired initial velocity field. Unfortunately, this scheme does not work very well. For example, it causes artificial orbit crossing in Lagrangian space (the same initial position for particles that are now in different places) because it tends to overestimate the velocities at early times (the Zel'dovich approximation typically underestimates the acceleration). Take, for example, a spherical void prior to shell crossing. The Zel'dovich approximation overestimates the radial velocities at early times, so some particles are predicted to come from across the center of the void. This may lead to severe errors in the initial density and velocity fields. One could reduce this problem by smoothing on a large scale, but this would be an unnecessary waste of small-scale information. Furthermore, the interpolation of the velocities from the discrete set of particles to a grid introduces large spatial variations that makes the differentiation to a density field difficult unless severe smoothing is applied. Finally, the coverage of Lagrangian space by the test particles could be very nonuniform.

Instead, we show below how the Zel'dovich approximation can be expressed in Eulerian space (of fixed positions) as a simple differential equation for a velocity-potential field. This equation does not involve the gravitational potential. It is a first-order equation which allows only a growing mode and could therefore be easily integrated backwards in time until convergence to the desired uniform initial state. The velocity and density fields could then be obtained by simple differentiation using linear theory.

There is an advantage in using the potential rather than the velocity or the density fields because, being a spatial integral of the velocity and double integral of the density, the potential suffers less from strong nonlinear effects which are most pronounced on small scales.

Assuming a potential flow, the natural outcome of gravitational instability, the present velocity-potential field can be extracted from observations in two independent ways. The observed radial peculiar velocities of galaxies (e.g., Lynden-Bell et al. 1988) could be integrated along radial rays via the POTENT method to give the velocity-potential field with associated error estimates (Bertschinger & Dekel 1989; Dekel, Bertschinger, & Faber 1990). The Zel'dovich approximation indeed guarantees that an artificial vorticity model is not generated during the integration back in time.

Under the Zel'dovich approximation, the velocity potential can also be obtained from the gravitational potential, which could be extracted from the observed distribution of galaxies in a whole-sky, complete redshift sample of galaxies, such as the *IRAS* samples (e.g., Strauss et al. 1990; Rowan-Robinson et al. 1990), under the assumption that galaxies trace the mass distribution. One has to integrate the Poisson equation, either in Fourier space or in configuration space (correcting for nonlinear effects).

The Eulerian Zel'dovich-Bernoulli equation is derived and discussed in § 2. The reconstruction method is tested using an N-body simulation in § 3. It is applied experimentally to real data in § 4 as an illustration of possible applications that will be discussed in an associated paper (Nusser, Dekel, & Bertschinger 1992). The method is discussed in comparison with other methods in § 5, and our results are summarized in § 6.

2. THE EULERIAN ZEL'DOVICH-BERNOULLI EQUATION

The common way of expressing the Zel'dovich approximation (Zel'dovich 1970) is by writing the displacement of each particle from its initial comoving $\boldsymbol{q}$ to its Eulerian comoving position $\boldsymbol{x}$ at time t as a product of a universal function of time, $D(t)$, and a time-independent perturbation function in Lagrangian space, $\psi(\boldsymbol{q})$, that is,

$$\boldsymbol{x}(\boldsymbol{q}, t) = \boldsymbol{q} + D(t)\boldsymbol{\psi}(\boldsymbol{q}) . \tag{1}$$

This means that the peculiar velocities of the particles all evolve in the same rate,

$$\boldsymbol{v}(\boldsymbol{q}, t) \equiv a(t)\frac{d\boldsymbol{x}}{dt} = a(t)\dot{D}(t)\boldsymbol{\psi}(\boldsymbol{q}) , \tag{2}$$

where $a(t)$ is the cosmological expansion factor.

What is $D(t)$? Using equation (1) and the continuity equation, the density fluctuation in the vicinity of each particle is given by $\delta(\boldsymbol{q}, t) = \bar{\rho}/J(\boldsymbol{q}, t) - 1$, where $\bar{\rho}$ is the mean comoving density and $J \equiv \| \partial \boldsymbol{x}/\partial \boldsymbol{q} \|$ is the Jacobian of the coordinate transformation. This turns out to be an exact solution of the equations of ideal-fluid cosmological fluctuations in the linear regime (i.e., as long as second-order terms in δ and $\boldsymbol{v}$ are negligible) with $\delta(t) \propto D(t)$ and where $D(t)$ is the growing-mode solution of the equation

$$\ddot{D} + 2H\dot{D} = \tfrac{3}{2}H^2\Omega D , \tag{3}$$

in which $H = \dot{a}/a$, and Ω is the time-dependent density parameter (e.g., Peebles 1980, eq. [11.1]). Therefore, if the growth of displacements is the same everywhere, it must be given by the same $D(t)$ under quasi-linear conditions as well. The Zel'dovich approximation differs from the linear approximation by taking into account particle displacements from their initial positions, so the density at a given position does not necessarily evolve according to the linear growth rate. In fact, infinite density can develop in a finite time as a result of convergence of particle trajectories into singular "pancakes."

Our goal here is to express the Zel'dovich approximation as a differential equation in Eulerian space where it could be integrated in time. The standard equation of motion of dust particles in an expanding universe is (e.g., Peebles 1980, eq. [7.12])

$$\frac{d\boldsymbol{v}}{dt} + H\boldsymbol{v} = -\frac{1}{a}\nabla\phi_g , \tag{4}$$

where ∇ is with respect to comoving positions and ϕ_g is the gravitational potential which obeys the Poisson equation at each position $\boldsymbol{x}$:

$$\nabla^2\phi_g = \tfrac{3}{2}H^2\Omega a^2\delta . \tag{5}$$

In order to see what the Zel'dovich approximation means in terms of the equation of motion, we make a coordinate transformation from the velocity and potential fields $\boldsymbol{v}(\boldsymbol{x}, t)$ and $\phi_g(\boldsymbol{x}, t)$ to the scaled fields

$$\mathfrak{V}(\boldsymbol{x}, t) \equiv \frac{\boldsymbol{v}(\boldsymbol{x}, t)}{a\dot{D}} \quad \text{and} \quad \varphi_g(\boldsymbol{x}, t) = \frac{\phi_g(\boldsymbol{x}, t)}{a^2\dot{D}} . \tag{6}$$

The equation of motion (4) then takes the form

$$\frac{d\mathfrak{V}}{dt} + \frac{3H\Omega}{2f(\Omega)}\mathfrak{V} = -\nabla\varphi_g , \tag{7}$$

where the standard definition of f has been used, $f(\Omega) \equiv$

$\dot{D}/(HD)$ ($\simeq\Omega^{4/7}$, Lightman & Schechter 1990; or $\simeq\Omega^{0.6}$, Peebles 1980).

In the Lagrangian interpretation, assuming *no orbit mixing*, $\boldsymbol{v}(\boldsymbol{x}, t)$ is the velocity at time t of *the* particle which is at position $\boldsymbol{x}$ at that time. If the motion were according to the Zel'dovich approximation, then, comparing equations (6) and (2), we would have $\mathfrak{V}(\boldsymbol{x}, t) = \psi(\boldsymbol{q})$ where $\boldsymbol{q}$ is determined by $\boldsymbol{x}$ and t via equation (1), that is, $\mathfrak{V}(\boldsymbol{x}, t)$ is the time-independent displacement corresponding to the particle which is at position $\boldsymbol{x}$ at time t. Thus, the Zel'dovich approximation of equation (2) is equivalent to the requirement

$$\frac{d\mathfrak{V}}{dt} = 0 , \tag{8}$$

where the derivative is along the trajectory of a given particle, $\boldsymbol{q}$ = const.

Using this approximation in equation (7), the velocity $\mathfrak{V}$ can be written as a gradient of a potential,

$$\mathfrak{V} = -\nabla\varphi_v , \tag{9}$$

where

$$\varphi_v(\boldsymbol{x}, t) = \frac{2f(\Omega)}{3H\Omega}\,\varphi_g(\boldsymbol{x}, t) + F(t) , \tag{10}$$

and where $F(t)$ is a function of time only. One can take F to be zero without loss of generality because what eventually matters are potential gradients. It is interesting to note that the Zel'dovich approximation automatically guarantees a potential flow with no vorticity (a manifestation of Kelvin's circulation theorem) and that the relationship between the gravitational and velocity potentials (10) is the same as in the linear approximation.

Using the convective derivative, $d/dt = \partial/\partial t + (d\boldsymbol{x}/dt)\cdot\nabla$, equation (7) corresponds in Eulerian space to

$$\frac{\partial\mathfrak{V}}{\partial t} + \dot{D}(\mathfrak{V}\cdot\nabla)\mathfrak{V} = 0 . \tag{11}$$

Then, using the vector identity $(\mathfrak{V}\cdot\nabla)\mathfrak{V} = (\frac{1}{2})\nabla\mathfrak{V}^2 - \mathfrak{V}\times(\nabla\times\mathfrak{V})$ and the no-vorticity property $\nabla\times\mathfrak{V} = 0$, one obtains

$$\nabla\left[\frac{\partial\varphi_v}{\partial t} - \frac{\dot{D}}{2}(\nabla\varphi_v)^2\right] = 0 . \tag{12}$$

Since one is free to add an arbitrary spatial constant to the potential, one can write without loss of generality

$$\frac{\partial\varphi_v}{\partial t} - \frac{\dot{D}}{2}(\nabla\varphi_v)^2 = 0 , \tag{13}$$

which we term the *Zel'dovich-Bernoulli* equation. Replacing the time variable t by $D(t)$ it takes the simple form

$$\frac{\partial\varphi_v}{\partial D} - \frac{1}{2}(\nabla\varphi_v)^2 = 0 . \tag{14}$$

Note that under the Zel'dovich approximation the two equations (10) and (13) replace the exact Bernoulli equation for a cosmological pressureless potential flow,

$$\frac{\partial\varphi_v}{\partial t} - \frac{\dot{D}}{2}(\nabla\varphi_v)^2 + \frac{3H\Omega}{2f(\Omega)}\,\varphi_v = \varphi_g . \tag{15}$$

[When the more familiar coordinates $\boldsymbol{v}$ and ϕ are used, the Bernoulli equation reads $\partial\phi_v/\partial t - a^{-2}(\nabla\phi_v)^2 = \phi_g$.]

3. TESTING THE METHOD WITH AN N-BODY SIMULATION

3.1. *Method*

Equation (14) is an extremely useful Eulerian representation of the Zel'dovich approximation. Given the potential field at some initial time this equation can be integrated forward or backward in time by simple numerical means. The equation is invariant under the transformation $D\rightarrow -D(t\rightarrow -t)$ and $\varphi_v\rightarrow -\varphi_v$, so integrating φ_v forward is analogous to integrating $-\varphi_v$ backward (φ_v and $-\varphi_v$ are statistically equivalent for a Gaussian random field initially).

The numerical time integration of equation (14) could be done in the most trivial way. Given φ_v at a certain time with some smooth boundary conditions, its gradient is calculated numerically. The equation then provides the time derivative of φ_v, which is used in a first-order Taylor expansion to predict the value of φ_v at the next, nearby time step. The equation is integrated this way from the present time, t_0, back to some initial time in the linear regime, t_i.

The velocity potential field at t_0 (the initial condition for the integration of eq. [14] backwards) can be computed from the velocity field at that time by spatial integration of equation (9). This integration could be easily performed in Fourier space, where the divergence of equation (9) corresponds to

$$\boldsymbol{k}\cdot\tilde{\mathfrak{V}}(\boldsymbol{k}) = -ik^2\tilde{\varphi}_v(\boldsymbol{k}) , \tag{16}$$

with $\tilde{\mathfrak{V}}(\boldsymbol{k})$ and $\tilde{\varphi}_v(\boldsymbol{k})$ the Fourier transforms of $\mathfrak{V}$ and φ_v. So to get the potential we first calculate $\nabla\cdot\mathfrak{V}$, then compute its Fourier transform, divide by $-ik^2$ according to equation (16), and Fourier transform back to configuration space. Periodic boundary conditions are imposed to allow the use of FFT.

The velocity potential at t_0 could also be computed from the density fluctuation field at that time. First, the gravitational potential is computed from $\delta(\boldsymbol{x})$ by solving the Poisson equation (5) in Fourier space,

$$\tfrac{3}{2}H^2\Omega a^2\,\tilde{\delta}(\boldsymbol{k}) = ik^2\tilde{\varphi}_g(\boldsymbol{k}) . \tag{17}$$

Then the velocity potential is given by equation (10).

Knowing the velocity potential at any given time one can obtain the corresponding velocity field by differentiation using equation (9), and then differentiate again to obtain the density-fluctuation field using the approximations we developed in Nusser et al. (1991, hereafter NDBB). In the linear regime the density is simply given by

$$\delta = -aD\nabla\cdot\mathfrak{V} . \tag{18}$$

3.2. *Simulations*

For testing the method we appeal to cosmological N-body simulations, using a standard particle-mesh code kindly provided to us by E. Bertschinger (Bertschinger & Gelb 1991; the same code that has been used in NDBB). We use 128^3 grid cells and 128^3 particles in a cubic comoving box of side $160h^{-1}$ Mpc with periodic boundary conditions. The grid spacing is thus 125 km s^{-1}—on the order of the comoving scale for a normal galaxy. Our study case started at $z = 100$ with a random realization of cold dark matter initial fluctuations (CDM; spectrum as in Davis et al. 1985), assuming $\Omega = 1$, $h = 0.5$, and normalizing such that the expected rms of $\delta M/M$ today is unity in spheres of radius $8h^{-1}$ Mpc based on linear theory (i.e., $b = 1$).

The output of the simulation at the final time is given as positions and velocities of the particles. Using cloud-in-cell interpolation (CIC) we calculate the density and velocity fields

at the points of the cubic grid (if the grid point resides in an empty cell, the velocity is interpolated from the nearest occupied cells). We then smooth the density and velocity fields further on a larger scale, using a spherical Gaussian window. Similar smoothing is required for the real universe by the sparse and noisy data, and it is necessary in general in order to smooth over regions of orbit mixing and too severe nonlinearities. In the simulations it helps avoiding local inaccuracies of the N-body code and the limited representation below the Nyquist wavelength.

3.3. *Zel'dovich versus True Initial Densities*

The Zel'dovich time machine described above is applied to the nonlinear velocity field of the N-body simulations at the final time, $\boldsymbol{v}(\boldsymbol{x})$, Gaussian smoothed with radius 500 or 1000 km s^{-1}. It yields an approximation to the initial field which we denote $\delta_Z(\boldsymbol{v})$. Alternatively, we apply the Zel'dovich time machine to the smoothed final density field of the simulation, $\delta(\boldsymbol{x})$, yielding the approximation $\delta_Z(\delta)$. The reconstructed density fields are compared with the true initial density field of the simulation, δ_I, smoothed in a similar way. We also refer to the present, Gaussian-smoothed density field, δ, and to the initial density reconstructed using linear approximations: either from the current density, that is, $\delta/(1+z)$, or from the current velocity, $\delta_d = -(D/\dot{D})\nabla \cdot \boldsymbol{v}$. For the comparison we scale the various density fields at the initial time (redshift z) by the linear growth factor $(1+z)$, so we always deal with fields of rms value of order unity.

First, in Figure 1, we show density-fluctuation contour maps in one arbitrary slice of the simulation. The densities refer to 1000 km s^{-1} Gaussian smoothing except that the Zel'dovich-reconstructed field marked $\delta_{Z8}()$ started by smoothing the current velocity field with a Gaussian of radius 800 km s^{-1} instead (to compensate for orbit crossing, as discussed below). The Zel'dovich reconstructions $\delta_{Z8}(\boldsymbol{v})$ and $\delta_Z(\delta)$ indeed provide a fairly good match to the true initial field, δ_I, everywhere. The linear approximations, both δ and δ_d, clearly tend to overestimate the density in the overdense regions and to underestimate the depth of the underdense regions. The overestimation of the initial overdensities reflects the fact that the linear approximation underestimates the actual nonlinear growth rate of positive density fluctuations. In the underdense regions, the error is mostly due to the fact that δ, by definition, cannot become smaller than -1, so the linear approximation, $\delta \propto (1+z)^{-1}$, can overestimate the growth rate of $|\delta|$ there.

Figure 2 shows point by point the different reconstructed densities against the true initial densities, δ_I, in 10^4 points chosen at random from the grid in the simulated volume. The errors made by the linear approximations at the high- and low-density ends are clearly seen, in agreement with the maps of Figure 1. They are more severe for the 500 km s^{-1} smoothing than for the 1000 km s^{-1} smoothing, as expected. The Zel'dovich reconstructions $\delta_Z(\boldsymbol{v})$ and $\delta_Z(\delta)$ show a tighter, quite *linear* correlation with the true initial field, which, to a certain extent, corrects the asymmetry between the positive and negative fluctuations introduced by nonlinear effects.

3.4. *On Smoothing and Crossing Streams*

This is a slight detour from the mainstream of the paper, which tries to clarify a nasty point of general concern. When the current velocities that enter the time machine are smoothed with a Gaussian of the same radius as used to smooth δ_I, the recovered $|\delta_Z(\boldsymbol{v})|$ typically underestimates $|\delta_I|$ by a constant

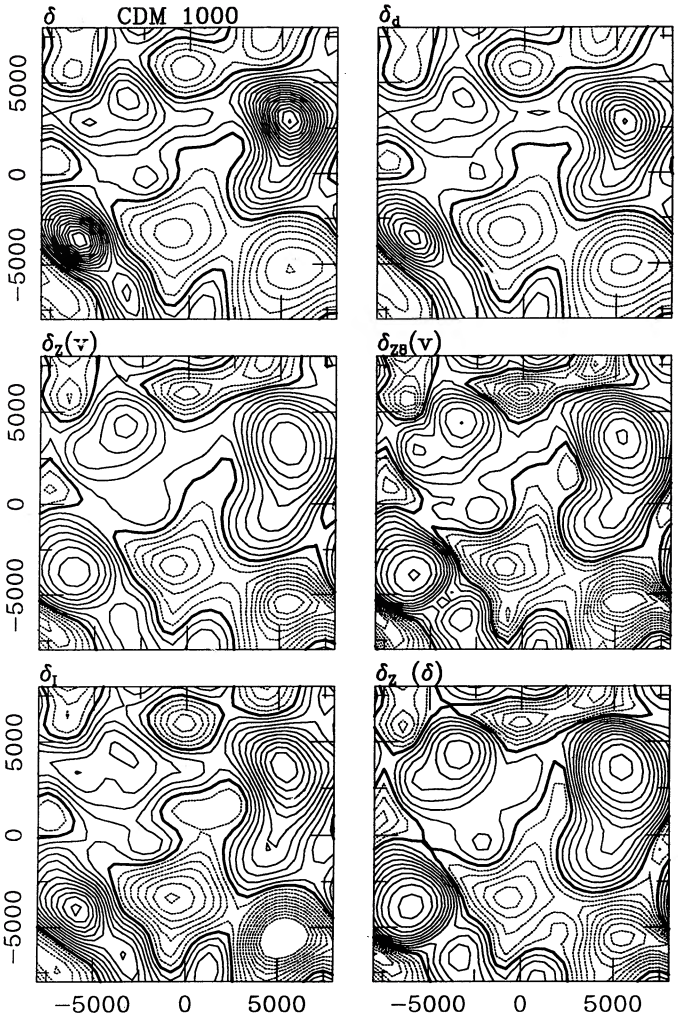

FIG. 1.—Initial density fluctuations at $z \sim 10^3$ in an arbitrary slice from a CDM N-body simulation ($b = 1$) with Gaussian smoothing of radius 1000 km s^{-1}. The zero contour is heavy, positive contours are solid, negative contours are dashed, and contour spacing is $0.1/(1+z)$. The true initial field is δ_I. The maps denoted δ_Z are the recovered Zel'dovich-Bernoulli approximations from the velocity and density, respectively, where δ_{Z8} is corrected for multistreaming. Upper panels show the fields recovered by linear approximations.

factor: 1.23 and 1.44 for 1000 and 500 km s^{-1} smoothing, respectively, determined by linear regression of $\delta_Z(\boldsymbol{v})$ over δ_I. Thus, the effective smoothing in the Zel'dovich reconstruction from the present $\boldsymbol{v}$ turns out to be larger despite the use of windows with the same size. Most of this systematic effect can be removed (at the expense of more scatter) by using a smaller smoothing radius for the velocities that are input to the Zel'dovich reconstruction. This is demonstrated in the middle-right plots of Figure 2, where 800 and 350 km s^{-1} velocity smoothings are used to compare with the 1000 and 500 km s^{-1} density smoothings, respectively.

The operation of (CIC and Gaussian) smoothing does not in general commute with the nonlinear operators in the equations governing the evolution of fluctuations, so this sort of discrepancy is expected. Our procedure recovers those initial fluctuations that would have led via exact gravity to the observed fluctuations smoothed at present. These recovered initial fluctuations are not necessarily the same as δ_I, the result of smoothing the true initial fluctuations at the initial time.

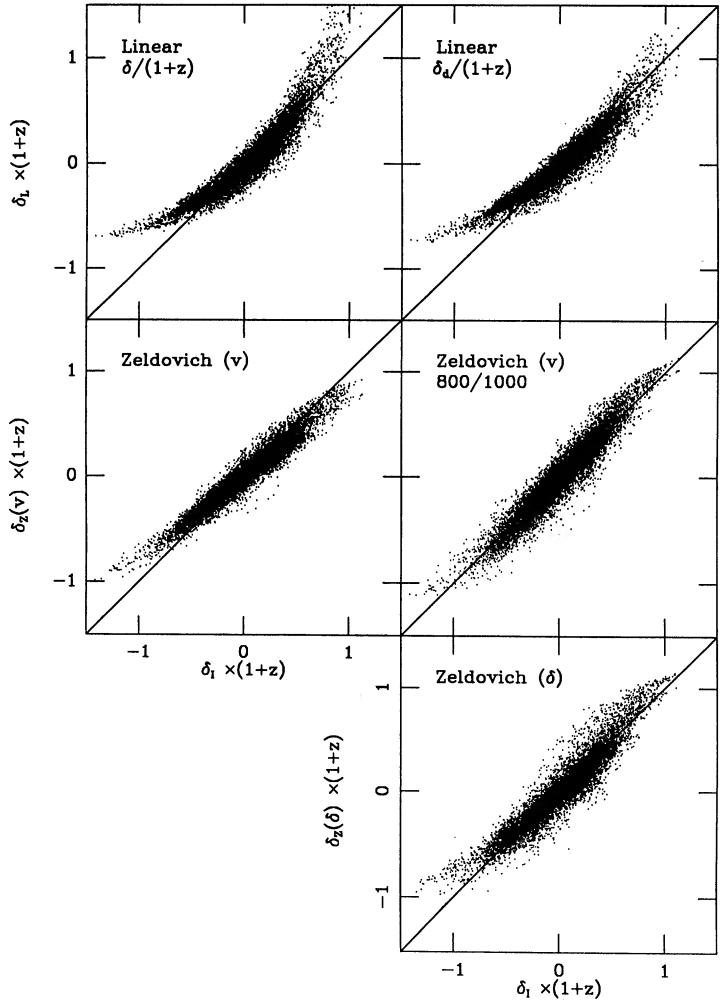

FIG. 2a

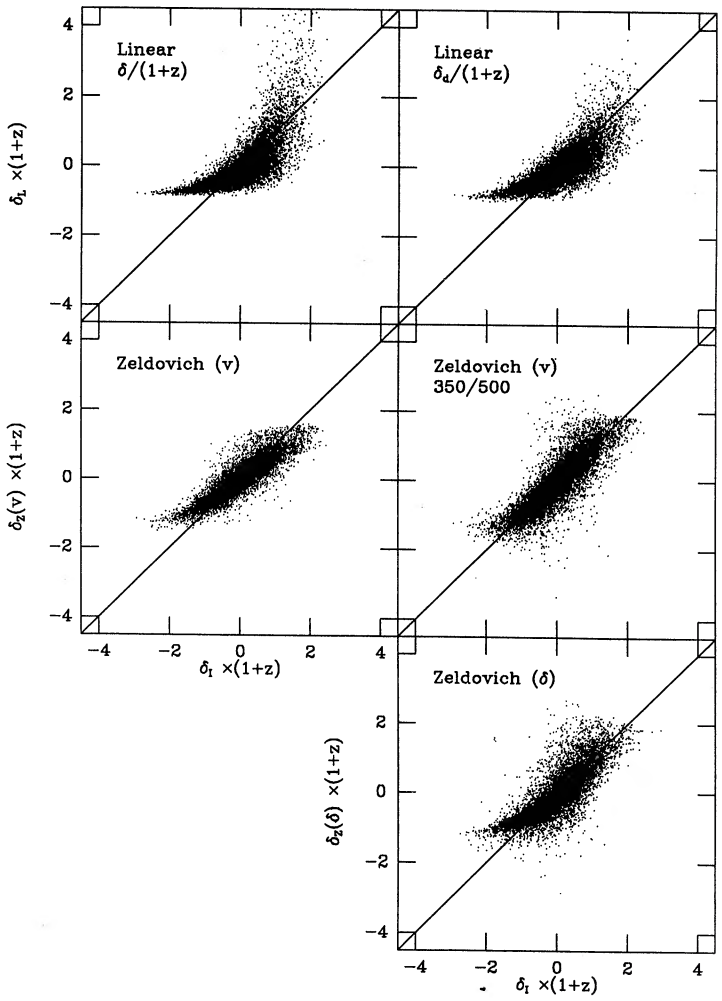

FIG. 2b

FIG. 2.—The recovered initial density-fluctuation fields vs. the true initial field in the simulation, point by point in a grid inside the simulated volume. The panels correspond to the panels in Fig. 1. The fields are Gaussian smoothed with a radius (*a*) 1000 km s^{-1} and (*b*) 500 km s^{-1}.

However, we find further that the smoothing has a stronger suppressing effect when applied to the velocities rather than the densities. This can be attributed mostly to regions where the velocity is a vector average over several streams. This effect has been noticed by NDBB, who found that the smoothed velocity derivatives in N-body simulations (where orbit crossing is present) tend to have lower amplitudes than those derived from exact solutions of symmetric configurations (spherical, cylindrical, and planar) with no orbit crossing.

The effect can be illustrated by the following toy model of one-dimensional collapse, where particle orbits are followed by the Zel'dovich approximation into and through a pancake. Figure 3 shows the velocity and density fields at an expansion factor 1.5 after the caustic formation. The initial velocity perturbation is a sine wave of length 2π. The particle velocities are interpolated by CIC into a grid of spacing $\pi/128$, and then Gaussian smoothed with $\sigma = 0.45$ (the half-pancake thickness at that time is 0.3). This provides the smoothed velocity field $v_s(x)$. The mass distribution is also interpolated and smoothed in the same way to provide $\delta_s(x)$. This smoothed density is compared to the density approximated from the smoothed velocity field via $\delta_d = -\nabla \cdot v_s$. The suppression of the smoothed velocity field and its gradient relative to the smoothed density near the peak where orbits cross is clearly seen.

If one wishes to get the normalization of the reconstructed field right, and not only the amplitudes of positive and negative fluctuations relative to each other, the additional effective smoothing due to multistreaming has to be taken into account when the input data are velocities, as in the POTENT analysis of observed velocities of galaxies. We considered two alternative ways to correct for this effect: (1) use for the input velocities the smoothing length desired for the density field but then multiply the reconstructed density fluctuation field by the constant correction factor deduced empirically from the N-body simulation (e.g., 1.23 for 1000 km s^{-1} smoothing), or (2) use an appropriately smaller smoothing length for the input velocity field (e.g., 800 km s^{-1} for the desired 1000 km s^{-1} smoothing of density). We use the former correction technique in the preliminary application of the method to the POTENT data in § 4. When the input data is density or potential field, the correction needed is smaller, and we ignore it in § 4.

3.5. *Spatial Distribution Function*

To compare the statistical properties of the recovered density fluctuations with the true initial conditions, consider first the one-point spatial distribution function, $P(\delta)$. The nonlinear density field develops a non-Gaussian distribution even when the initial fluctuations are a random Gaussian field (see Kofman et al. 1992). The asymmetry between positive and negative fluctuations (as measured by the skewness, for example), could be intuitively attributed to (1) the fact that positive fluctuations tend to contract and therefore to occupy less volume at later times while negative fluctuations typically expand to occupy larger volumes, hence shifting the peak of the distribution toward negative δ-values, (2) the tendency of nonlinear fluctuations in collapsing regions to grow faster than linear fluctuations, producing a tail at the positive end, and (3) the lower limit $\delta \geq -1$ imposed by definition, which introduces a noticeable cutoff in nonlinear systems.

Figure 4 shows the spatial distributions of the various density fluctuation fields of the N-body simulation for the different smoothing lengths. In the figures, all the δ are normalized by the standard deviation, $\sigma \equiv \langle(\delta - \langle\delta\rangle)^2\rangle^{1/2}$, of the present density field, δ. The linear-linear plot focuses on the central peak region, while the $\ln P - \delta^2$ plot stresses the tails of the distribution. In order to quantify the deviation from a normal distribution, Table 1 lists the skewness (S) and kurtosis (K) relative to the mean of each of these distributions, defined by

$$S \equiv \frac{\langle(\delta - \langle\delta\rangle)^3\rangle}{\sigma^3} \quad \text{and} \quad K \equiv \frac{\langle(\delta - \langle\delta\rangle)^4\rangle}{\sigma^4} - 3 . \quad (19)$$

For reference, a Gaussian distribution has $S = K = 0$. The distribution of the true initial field in the simulation, δ_I, is indeed close to a Gaussian by construction. The nonzero moments of δ_I can serve as rough estimates for the errors due to the limited volume sampled. The developed skewness of the distribution of the nonlinear δ is very apparent, as expected. With 500 km s^{-1}

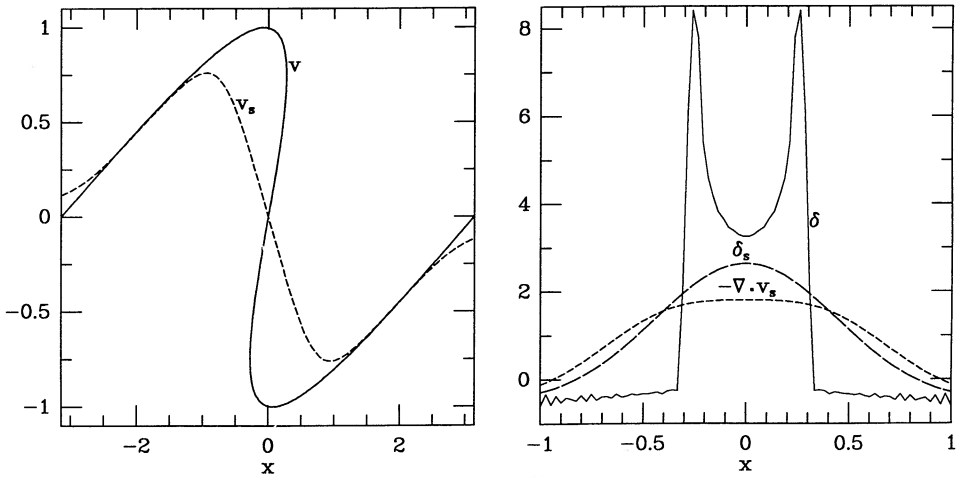

FIG. 3.—The effect of multistreaming in a one-dimensional pancake. *Left*: particle velocities v and the smoothed velocity field v_s (CIC and Gaussian smoothing). *Right*: exact density contrast δ, smoothed density contrast δ_s (CIC and Gaussian smoothing), and the density contrast derived from the smoothed velocity field, $-\nabla \cdot v_s$.

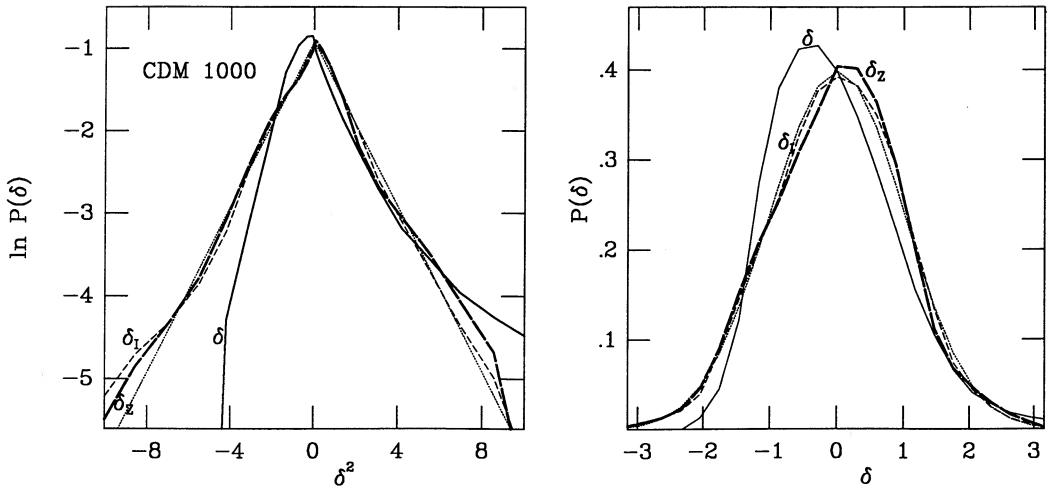

FIG. 4*a*

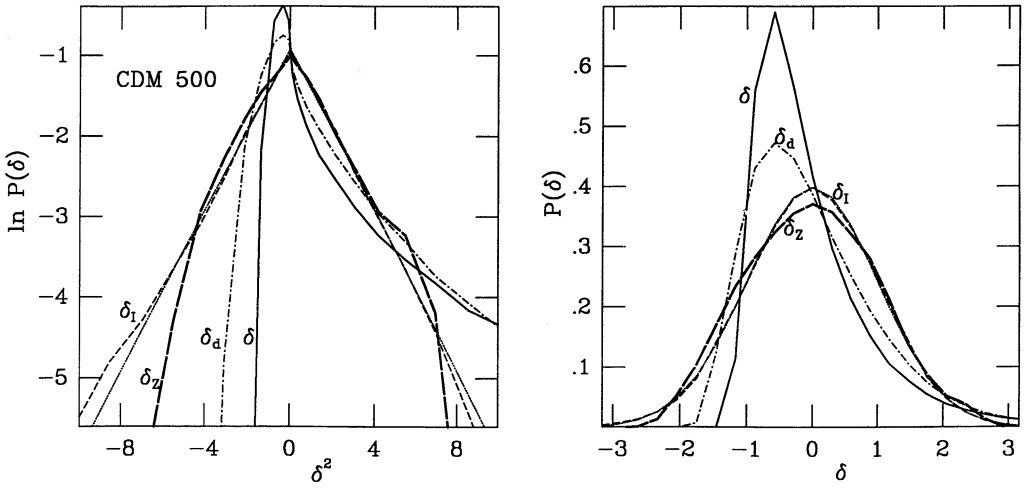

FIG. 4*b*

FIG. 4.—Spatial distribution function of density fluctuations in the recovered vs. true initial fields. The same data is shown as a linear plot (*right*) and as $\ln P - \delta^2$ (*left*) to stress different parts of the distribution. The different approximations are marked as in Figs. 1 and 2. The dotted curve is a Gaussian, with which the true initial distribution, δ_I, almost coincides. The fields are Gaussian smoothed with a radius (*a*) 1000 km s^{-1} and (*b*) 500 km s^{-1}.

smoothing we have $S \simeq 2.5$ and $K \simeq 11$. Recall that the same moments apply to the initial field that is reconstructed assuming linear theory. The distribution of the initial field reconstructed by the Zel'dovich scheme of this paper, $\delta_Z(\boldsymbol{v})$, quite successfully recovers the initial Gaussian distribution, with $S \simeq 0.1$ and $K \simeq 0.5$. This is an encouraging confirmation for the success of the method because the Gaussianity has not been imposed in any direct way.

TABLE 1

MOMENTS OF DENSITY DISTRIBUTION IN A CDM SIMULATION

Variable	Smoothing	$\sigma(1+z)$	Skewness	Kurtosis
Gaussian	...	...	0.000	0.000
δ	500	0.708	2.498	11.008
δ_d	500	0.514	0.946	1.158
$\delta_Z(v)$	500	0.581	0.107	−0.465
$\delta_{Z35}(v)$	350	0.792	0.132	−0.523
$\delta_Z(\delta)$	500	0.705	0.572	−1.350
δ_I	500	0.755	−0.065	0.015
δ	1000	0.325	1.021	2.059
δ_d	1000	0.250	0.376	−0.080
$\delta_Z(v)$	1000	0.287	−0.033	0.033
$\delta_{Z8}(v)$	800	0.367	0.019	−0.107
$\delta_Z(\delta)$	1000	0.342	0.308	0.165
δ_I	1000	0.345	−0.103	0.135

3.6. *Power Spectrum*

A complementary statistic is the power spectrum of the fluctuations, P_k (or, equivalently, the two-point correlation function). One could naively expect the nonlinear evolution to modify the shape of P_k after it has been constant throughout the linear evolution. Figure 5 shows the power spectra for the different density fluctuation fields of the N-body simulation, for the two smoothing lengths. It is computed by averaging the squares of the amplitudes of the Fourier transforms at given values of wave-vector length in bins $(k, k + \Delta k)$. Somewhat surprisingly, δ and δ_I turn out to be remarkably similar in shape over the range of scales under consideration. The nonlinear effects on the spectrum, for the quasi-linear smoothed system studied here, are only secondary. This can be qualita-

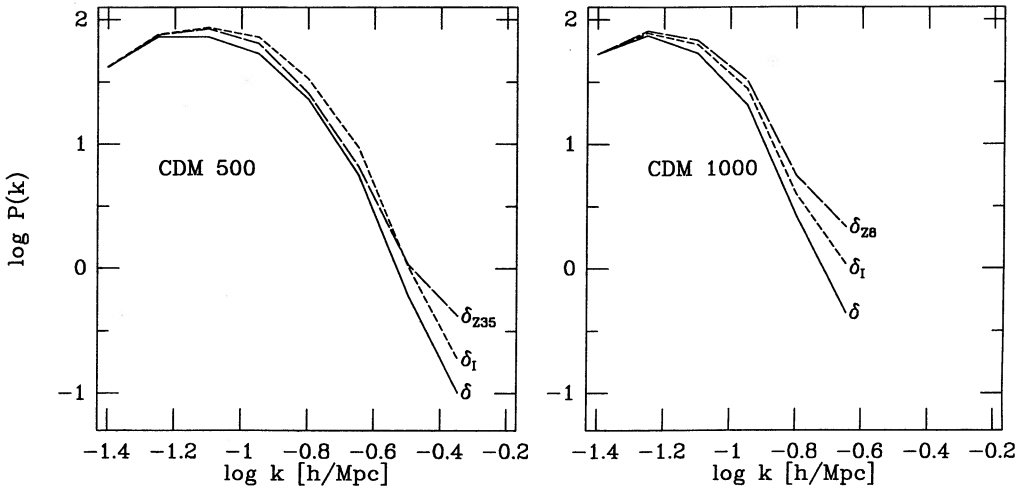

FIG. 5.—Power spectra in the recovered vs. true initial density fluctuation fields. The different approximations are marked as in Figs. 1, 2, and 4. The fields are Gaussian smoothed with a radius (*a*) 1000 km s^{-1} and (*b*) 500 km s^{-1}.

tively understood as follows. While positive fluctuations speed up their growth (relative to linear growth) during collapse, they slow down after virialization.

Furthermore, the growth of negative fluctuations always slows down when they get close to the emptiness limit $\delta = -1$. These competing effects apparently cancel each other and leave the smoothed spectrum almost unchanged. The numerical technique used to compute the spatial derivatives in the Zel'dovich-Bernoulli equation plus the inaccuracies of the PM code on scales of a few grid cells are responsible for an apparent discrepancy on scales below the smoothing length outside the range shown in the figure. We conclude that for a spectrum close to a CDM-modified Harrison-Zel'dovich spectrum, a nonlinear time machine is not really needed for the recovery of the initial power spectrum. However, this result might be specific to this kind of spectrum. The time machine will be tested with other spectra elsewhere.

4. PRELIMINARY APPLICATION

The method discussed above is applied to real data in an associated paper. Here we just bring a preliminary, qualitative application in order to demonstrate the effectiveness of the method.

The input data to the Zel'dovich time machine are either the velocity potential field recovered from the observed velocities by the POTENT procedure (Dekel et al. 1990; Bertschinger et al. 1990a), or the density field derived from the distribution of *IRAS* galaxies (Strauss et al. 1992).

The POTENT potential, after smoothing the velocities with a Gaussian of radius 1200 km s^{-1}, is provided on a grid of 500 km s^{-1} spacing inside a sphere of radius 7000 km s^{-1} about the Local Group. The boundary conditions for the Zel'dovich-Bernoulli equation were chosen arbitrarily to be $\nabla^2\varphi = 0$ outside of this sphere. The recovery procedure assumed $\Omega = 1$. The reconstructed density fluctuation field was multiplied by the empirical correction factor 1.2 to compensate for the additional smoothing in the POTENT velocity smoothing procedure due to orbit crossing. The current and recovered initial density fields in the supergalactic plane out to 6000 km s^{-1} from the Local Group are presented in Figure 6 as contour maps.

Note that the huge overdensity at the bottom of the plot, the features at the bottom left, and the underdense region at the right edge (this is the vicinity of the Perseus cluster), are clearly noise features that are artifacts of the poor sampling of the velocity field in these regions combined with large distance measurement errors (Dekel et al. 1990; Bertschinger et al. 1990a). The major features of the Great Attractor at the upper-left quadrant, the big void in the lower half, and the overdensity at the lower-right quadrant (the Pisces part of the Perseus-Pisces supercluster) are trustworthy; in most of these regions the error in δ is typically 0.2 (and is less than 0.4).

The Zel'dovich time machine affects the density field as it did in the *N*-body simulation test. The zero fluctuation contour remains the same, and the same main features show up, except that their relative contrast changes. The peak of the Great Attractor (with 1200 km s^{-1} smoothing) is down from $\delta = 1.5$ today to $\delta_z = 1.0/(1 + z)$ in the linear regime. The center of the big void is down from $\delta = -0.4$ today to $\delta_z = -0.6/(1 + z)$ in the linear regime. Pisces is down from $\delta = 0.8$ to $\delta_z = 0.6/(1 + z)$.

The *IRAS* input data is the density field within 8000 km s^{-1} (Strauss et al. 1992), as derived from a redshift sample of *IRAS* galaxies (Strauss et al. 1990), each weighted inversely with the observational selection function at that position. The mean density is computed within the sampled volume. The mass density fluctuation field is assumed to be the same as that of the *IRAS* galaxies, that is, no biasing. The density fluctuation field is zero-padded outside this sphere filling a cubic box of side 16,000 km s^{-1} with periodic boundary conditions. The gravitational potential is derived by solving the Poisson equation in Fourier space (17), and the velocity potential is calculated using equation (10).

The effects on the *IRAS* density map are qualitatively similar to the effects on the POTENT maps. The Great Attractor and Perseus-Pisces peaks are down from $\delta = 0.8$ today to $\delta_z = 0.6/(1 + z)$ early on, and the big void is down from $\delta = -0.4$ to $\delta_z = -0.6/(1 + z)$.

5. DISCUSSION: COMPARISON WITH OTHER METHODS

The problem of tracing the fluctuations of a gravitating system back in time is in principle a problem of mixed boundary conditions. In general, we are given certain information about the dynamical fluctuation fields (density, velocity,

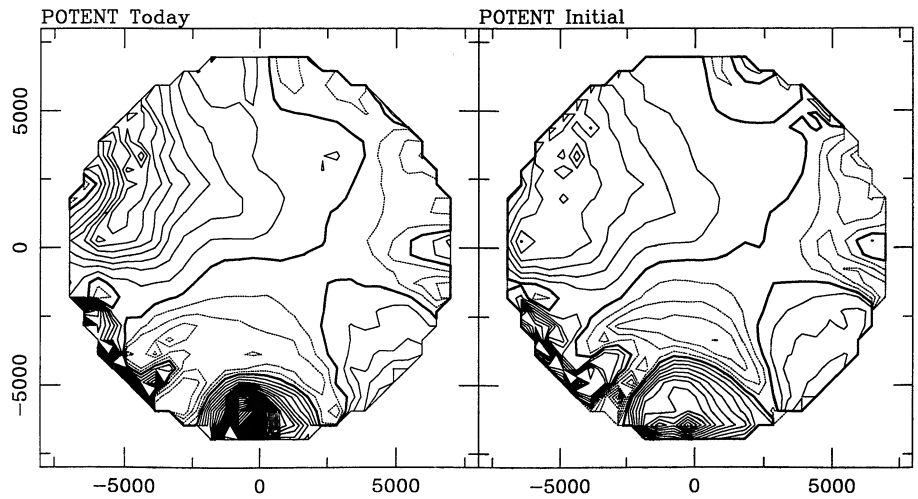

FIG. 6.—POTENT initial vs. present mass density fluctuation fields in the supergalactic plane. The present mass density is extracted from observed velocities via POTENT by Dekel et al. (1990) and Bertschinger et al. (1990a). The initial conditions are recovered by the method of this paper [$\delta_Z(v)$]. The smoothing radius is 1200 km s^{-1}, and a multistreaming correction factor of 1.2 is applied. The zero contour is heavy, positive contours are solid, negative contours are dashed, and contour spacing is $0.2/(1 + z)$.

potential) at a final time t_0, and we require that the fluctuations are very small at an initial time, t_i. (Note that the relationship between the present nonlinear velocity and density fields, e.g., NDBB, also involves the constraint of smooth initial conditions.)

In the method described here we replace the requirement of smooth initial conditions with the restriction to a *growing* mode via the Zel'dovich approximation which we apply in an Eulerian new version. The *Ansatz* of *potential* flow allows us to compute a velocity potential field from the nonlinear velocity or density fields at t_0, which can then be integrated back in time as a simple initial-value problem. The potential flow is predicted by linear gravitational instability theory and is preserved by the Zel'dovich approximation as long as orbit crossing is negligible or could properly be smoothed over.

A brief review of other methods might be useful here. One idea is to explicitly enforce *Gaussianity* on the initial conditions (Weinberg 1992). The method is based on the assertion (partly tested by simulations) that nonlinear deviations from an initial Gaussian distribution of fluctuations in Eulerian cells preserve the ranking of cells by density. For example, it assumes that the movement of peaks could be ignored. The nonlinear, non-Gaussian distribution of density fluctuations in cells is first "Gaussianized" in a rank-preserving way and then evolved back in time using linear theory. In practice, this procedure requires a model-dependent correction procedure. This method has been applied to a galaxy redshift survey in the Perseus-Pisces region, suggesting, for example, a biasing factor of order $b \simeq 2$ for convergence to a self-consistent solution (Weinberg 1992). This method is restricted to the case of Gaussian initial fluctuations, and the data at t_0 must be a density field because the velocity field does not develop strong deviations from a Gaussian distribution (Kofman et al. 1991).

Peebles (1989) reminded us of Hamilton's principle: when the mass distribution is modeled by a set of particles whose possible orbits are parameterized, the orbit parameters can be

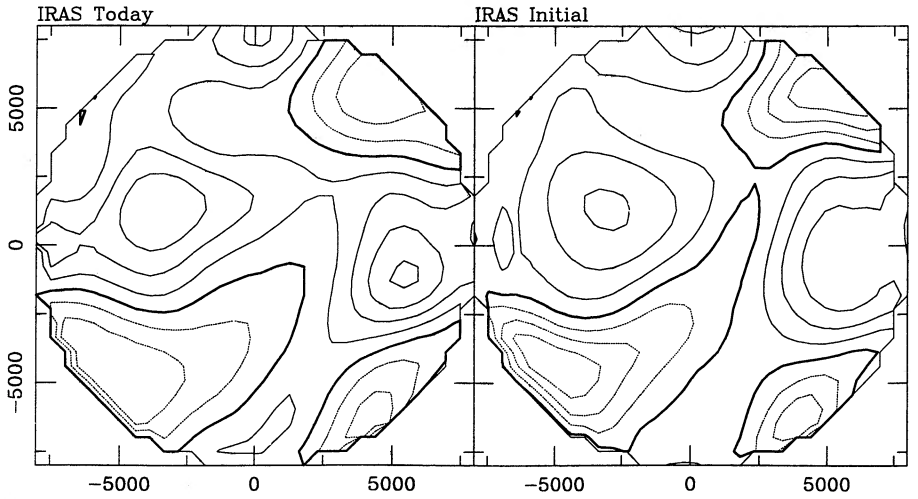

FIG. 7.—*IRAS* initial vs. present mass density fluctuation fields in the supergalactic plane. The present mass density is extracted from the observed distribution of *IRAS* galaxies by Strauss et al. (1992). The initial conditions are recovered by the method of this paper [$\delta_Z(\delta)$]. The smoothing radius is 1200 km s^{-1}. The zero contour is heavy, positive contours are solid, negative contours are dashed, and contour spacing is $0.2/(1 + z)$.

chosen by minimizing an *action* subject to the constraints at the initial and final times. Peebles used this method to determine the trajectories of galaxies in the Local Group, given their present positions. By comparing the predicted and observed velocities, he concluded that the Local Group could indeed be a product of gravity and that a low value of Ω is favored.

Yahil and his colleagues (1992) have recently extended the minimum-action scheme by choosing a natural parameterization for the orbits which seems to improve the convergence to the desired solution. They generalized the Zel'dovich approximation (1) to a series expansion of the displacements in powers of D to an arbitrary order (n). The scheme was tested in the case of spherical collapse and found to converge rapidly to the exact solution (practically, with $n = 4$). They also formulated this scheme in Eulerian space using a Hamiltonian field theory of gravity, with integration over space replacing summation over particles.

These promising minimum-action schemes still need to overcome certain difficulties before they can be applied to a general gravitating system. For example, convergence is not a priori guaranteed in the general case, and even if the procedure converges, it may converge to an unwanted solution out of several possible solutions to the nonlinear system of equations. There is a hope that in the case of a laminar flow the system would usually converge to an exact solution, but, unfortunately, realistic cosmological flows do contain orbit crossings at some level. Even in slightly nonlinear systems the operation of spatially smoothing the fields does not necessarily commute with the nonlinear operators in the equations governing the evolution of fluctuations. The "exact" solutions are therefore not particularly useful for observed systems, where smoothing must be applied. Lagrangian schemes are hard to adjust, but Eulerian schemes can be corrected in several ways to account for multistreaming (e.g., § 3.4 and NDBB). Any scheme for recovering the initial conditions of the real universe should try to meet the challenge imposed by multistreaming.

The approximate method of this paper has the advantages that it is extremely simple to implement, it is easy to correct for smoothing over multistreams, and it is satisfactorily accurate in comparison with the measurement errors.

6. SUMMARY

We enforce smooth initial conditions by limiting the evolution of fluctuations to the growing mode, and we enforce gravity by assuming a potential flow and the Zel'dovich approximation. By scaling the Eulerian peculiar velocities inversely with $\dot{D}$ (eq.[6]), we find that for Zel'dovich trajectories (eqs. [1], [2], and [8]) the Bernoulli equation (15) is split into two: one part confirms that the velocity is derived from a potential (eqs. [9]–[10]), and the other is a first-order equation for this potential that can be easily integrated back in time in Eulerian space (eq. [13]). The velocity potential today is computed either from the velocity field (e.g., as provided by the POTENT analysis of observed radial velocities) or from the density field (e.g., as deduced from an *IRAS* redshift survey assuming that galaxies trace mass) by integrating eqs. (9) or (5–6), respectively.

The method is tested with an N-body simulation of Gaussian, $\Omega = 1$, CDM initial conditions, where the initial and final conditions are fully known. With Gaussian smoothing of 500 and 1000 km s^{-1}, the quasi-linear scheme is doing significantly better than the linear approximation in several ways. In particular, the scheme recovers quite well the initial Gaussian distribution of density fluctuations. Given the present velocity or density fluctuation fields, the recovered densities at the initial conditions are lower then the prediction of linear theory; the hills are lower and the valleys are deeper. For example, at the peak of the Great Attractor, with 1200 km s^{-1} smoothing, the reduction is by about 40%. The power spectrum, at least for the standard CDM spectrum studied, is not affected much by nonlinear evolution in the quasi-linear regime.

This method provides one more useful component to the family of methods for recovering the initial dynamical fluctuation fields at $z \sim 10^3$ from present observations. In an associated paper (Nusser & Dekel 1992), we describe a specific method for recovering the initial probability distribution function and explore its Ω-dependence. Using independent data for density and velocity we are able to determine both the initial distribution and Ω.

We thank E. Bertschinger for his PM code. We thank our POTENT collaborators for allowing the use of POTENT output for the preliminary illustration in Figure 6, and A. Yahil for providing the *IRAS* data of Strauss et al. (1992) used as an illustration in Figure 7. We are grateful for stimulating discussions with E. Bertschinger, J. Primack, D. Weinberg, and S. White. This research has been supported by US-Israel Binational Science Foundation grant 89-00194.

REFERENCES

Bertschinger, E., & Dekel, A. 1989, ApJ, 336, L5
Bertschinger, E., Dekel, A., Faber, S. M., Dressler, A., & Burstein, D. 1990a, ApJ, 364, 370
Bertschinger, E., & Gelb, G. 1991, Computers in Physics, 5, 164
Bertschinger, E., Gorski, K., & Dekel, A. 1990b, Nature, 345, 507
Davis, M., Efstathiou, G., Frenk, C., & White, S. D. M. 1985, ApJ, 292, 371
Dekel, A., Bertschinger, E., & Faber, S. M. 1990, ApJ, 364, 349
Efstathiou, G., Kaiser, N., Saunders, W., Lawrence, A., Rowan-Robinson, M., Ellis, R. S., & Frenk, C. S. 1990, MNRAS, 247, 10P
———. 1991, ApJ, submitted
Kofman, L., Gelb, J., Bertschinger, E., Nusser, A., & Dekel, A. 1992, preprint
Lightman, A., & Schechter, P. 1990, preprint
Lynden-Bell, D., Faber, S. M., Burstein, D., Davies, R. L., Dressler, A., Terlevich, R. J., & Wegner, G. 1988, ApJ, 326, 19
Nusser, A., & Dekel, A. 1992, in preparation
Nusser, A., Dekel, A., & Bertschinger, E. 1992, in preparation
Nusser, A., Dekel, A., Bertschinger, E., & Blumenthal, G. 1991, ApJ, 379, 6 (NDBB)
Peebles, P. J. E. 1980, The Large-Scale Structure of the Universe (Princeton: Princeton Univ. Press)
———. 1989, ApJ, 85, 801
Rowan-Robinson, M., et al. 1990, MNRAS, 247, 1
Strauss, M. A., Davis, M., Yahil, A., & Huchra, J. P. 1990, ApJ, 361, 49
———. 1992, ApJ, 385, 421
Weinberg, D. 1992, MNRAS, submitted
———. 1992, in preparation
Yahil, A., et al. 1992, in preparation
Zel'dovich, Ya. B. 1970, A&A, 5, 20